OPTICAL CHARACTERIZATION OF QUANTUM DOT INTERMEDIATE BAND SOLAR CELLS

E. Cánovas, A. Martí, D. Fuertes Marrón, E. Antolín, P.G. Linares and A. Luque

Instituto de Energía Solar - Universidad Politécnica de Madrid
ETSI Telecomunicación, Ciudad Universitaria sn, 28040 Madrid – Spain
Phone: +34 915495700, email: canovas@ies-def.upm.es

C.D. Farmer and C.R. Stanley

Department of Electronics and Electrical Engineering
University of Glasgow, Glasgow G12 8QQ, Scotland - UK

ABSTRACT: In this paper we present an optical characterization for quantum dot intermediate band solar cells (QD-IBSCs). The cells were developed by growing a stack of ten InAs/GaAs QDs layers between p and n doped GaAs conventional emitters. Electroluminescence, EL, photoreflectance, PR, and transmission electron microscopy, TEM, were applied to the samples in order to test and characterize them optically. The results, derived from the application of the different techniques, showed a good correlation. TEM images revealed a very good structural quality of the QDs, which seem to evolve in shape-strain from the bottom to the top of the stack. Corresponding to the quality observed by TEM, strong signals from EL and PR resolved unambiguously the energy band diagram of the QD-IBSCs. By fitting PR data we were able to indentify the coexistence of bands and discrete energy levels coming from the IB material. The PR data evidenced also a strong electric field over the dots, attributed to the space charge region created between the p-n emitters sandwiching the IB material. From EL results, we identified the predominantly radiative nature of the IB material related energy transitions.
Keywords: Intermediate Band, Quantum Dots, Spectroscopy

1 INTRODUCTION

The intermediate band solar cell (IBSC) has been proposed in order to increase notably the conversion efficiency in photovoltaic's devices [1]. The better efficiency of such IBSCs, when compared with other technologies, relies on two basics: (i) increase the SC photocurrent by below fundamental band-gap photon absorption assisted by the presence of the intermediate band and (ii) a SC output voltage limited by the VB→CB energy transition of its energy band diagram.

The IBSCs have been theoretically modeled and practically implemented by sandwiching a stack of quantum dots (QDs) between conventional p and n emitters (QD-IBSCs). Operating as solar cells, the QD-IBSCs have not shown yet the predicted improved efficiency performance when compared with reference samples without IB material. This fact has been explained theoretically arguing different problems and deviations from the ideal model [2]. For this reason, and being the IB concept relatively new, it is worthy to study and characterize the properties of the QD-IBSCs by the application of conventional emission and absorption based spectroscopy techniques. In this way, this paper will show, analyze and discuss the combined results derived from the application of electroluminescence (EL), photoreflectance (PR), and transmission electron microscopy (TEM) on several QD-IBSCs samples.

2 EXPERIMENTAL

The samples were made at Glasgow University by molecular beam epitaxy (MBE). The QDs forming the IB material were grown on SI-GaAs by the so called Stranski-Krastanov growth mode [3]. In this mode, the QDs appear spontaneously over an extremely thin quantum well (known as wetting layer, WL) due to strain relaxation induced by the different lattice constants of dot (InAs) and barrier (GaAs) material. In order to increase the volume of IB material and hence its absorption, up to ten layers of InAs/GaAs QDs were stacked on the samples considered here, see fig. 1. Each layer of QDs was grown, at T=530ºC, depositing 2.7monolayers (MLs) of InAs and capped with 10 nanometers of GaAs working as barrier material. To allow the pumping of carriers from the IB to the conduction band, CB, half-filling the IB is necessary. In this respect, every layer of QDs was delta-doped with $[Si] \approx 4 \cdot 10^{10} cm^{-2}$.

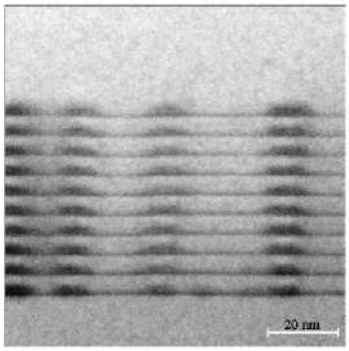

Figure 1: TEM image showing p (top) and n (bottom) emitters sandwiching the IB material. The IB is composed by a ten layer stack of InAs/GaAs QDs. Thin InAs WLs supporting the QDs and some small dots, located in the seed layer which do not progress in the stack, are also revealed by TEM.

After the growth, some pieces of 2x2 mm^2 were encapsulated as SCs with front and back metal contacts.

These samples were characterized by EL applying a forward bias current up to one amp. The luminescence light output was collected by lenses and focused into a VIS-NIR spectrometer coupled to a germanium detector. Other pieces of the resulting wafer were reserved without metallization for PR characterization. Using a conventional PR setup [4], the light (probe beam) coming from a 250W Quarz lamp was spectrally decomposed by a 1/8m monochromator. The resulting monochromatic beam was reflected over the sample and detected by a Ge detector. A HeNe (632nm, 17mW) laser beam (pump beam), mechanically chopped at 777Hz, was focused coinciding with the spot of the probe beam. The change in reflectivity due to the modulated beam was measured by a lock-in amplifier, after that, the resulting data was recorded by a computer.

3 RESULTS AND DISCUSSION

Figure 2 shows a comparison of characteristic room temperature EL and PR signals for a QD-IBSC. Both signals reveal different contributions realted to the QDs, WLs and barrier material (substrate). PR signal also shows several Franz-Keldysh oscillations (FKOs) over GaAs fundamental bandgap energy. EL signal by itself is not able to resolve clearly the number of energy transitions involved. However we can decompose EL signal in different Gaussians contributions assisted by the information extracted from PR, see fig. 3. As noted in fig. 2, the PR spectrum presents at least 4 contributions from the InAs QDs, denoted from QD0 to QD3. Also PR reveals 2 peaks for the WLs hosting the dots, and a larger contribution related to the barrier-substrate material. These transitions will be analyzed separately later.

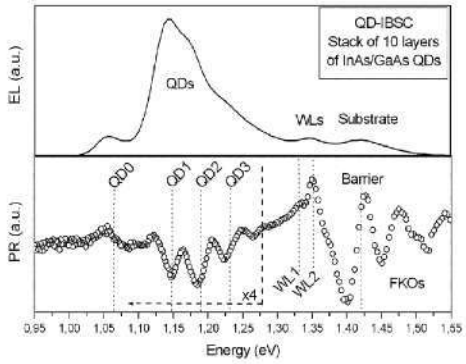

Figure 2: Characteristic EL and PR spectra for a QD-IBSC. For comparison purposes, EL was shifted against a Stokes effect.

Figure 3 presents the fitting to the EL spectra. The data extracted from the fitting can be found in Table I. The whole feature shows a low energy shift when compared with PR data. This shift is attributed to a Stokes shift observed previously for QDs based similar samples [5]. The EL data evidence a lower density of states (DOS) for the ground state QD0 compared with the excited ones, in agreement with published results [6]. In order to achieve a proper fitting for the QDs, it is necessary to include a broad extra feature as a baseline around 1.2eV. This feature has sense attending to the contribution of QDs located in the stack which deviate in size from the main population. For example, as Fig. 1 shows, some small QDs do not progress in the stack. Other of our EL results, not published yet, for samples with only one QD layer and emission around 1.2eV, invite us to consider also the signal from the QDs seed layer (the first layer of the stack) to contribute to this extra feature in EL. The reason for this consideration relies on the fact that the governing strain pattern around the dots in successive layers is different. For the seed layer the growth of the QDs is mainly governed by the different lattice constants of dot-barrier materials. However, for the upper layer in the stack the strain contribution of the preceding buried islands become dominant in the growth [7].

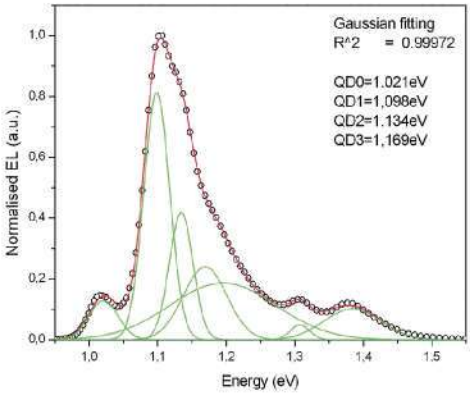

Figure 3: Fitting to the EL signal of a QD-IBSC.

Figure 4 shows the fitting for the PR data related to the absorption of the InAs QDs. Table I (bottom) shows the different figures obtained.

Table I: Values obtained from fitting EL and PR spectra.

EL	Energy (eV)	FWHM
QD0	1.021	0.042
QD1	1.098	0.037
QD2	1.134	0.034
QD3	1.169	0.063
QD	1.195	0.154
WL	1.307	0.028
GaAs	1.384	0.082

PR	Energy (eV)	Γ	m
QD0	1.065	0.035	1.8±0.4
QD1	1.150	0.025	2.6±0.1
QD2	1.187	0.032	2.4±0.1
QD3	1.227	0.027	2.5±0.1
WL1	1.327	0.042	2.5±0.1
WL2	1.362	0.032	2.5±0.1
GaAs	1.423	0.086	2.5±0.1

By fitting the PR features using the Aspnes generalized derivative form [8] (eq. 1) we can extract valuable information about the carrier confinement [9],

$$PR = \mathrm{Re}\left(\sum_{j=1}^{p}\left[C_j e^{i\theta_j}\left(E - E_{g,j} + i\Gamma_j\right)^{-m_j}\right]\right), \qquad (1)$$

where p is the number of spectral features in the region to be fitted, C_j, θ_j, $E_{g,j}$ and Γ_j are the amplitude, phase, gap energy and broadening parameter respectively of the jth structure. m_j depends on the nature of the critical point and order of the derivative, i.e., m=2 corresponds to the first-derivative of a Lorentzian, m=2.5 to the third-derivative of a 3D parabolic critical point (CP). First-derivative line shapes are obtained for bound states (such as isolated QWs) where the carriers cannot be displaced in the direction of the perturbation (electric field). In this case the translational symmetry of the crystal is preserved. Third-derivative line shapes appear when the modulated electric field destroys the translational symmetry of the sample as a consequence of the displacement of carriers. Third-derivative line shapes indicate un-confinement of the carriers involved.

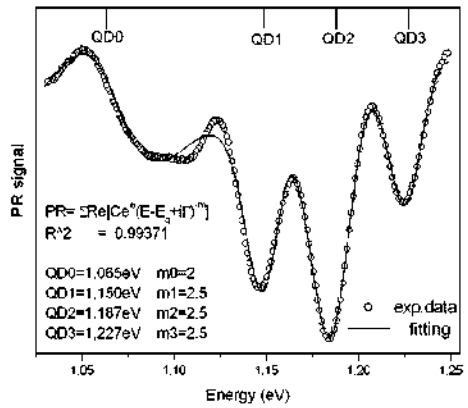

Figure 4: PR fitting procedure for QDs related signal in a QD-IBSC.

As shown in Fig. 4 and noted in Table I, only the QD0 ground state transition presented, because its fitted m_0 value, vertical confinement of the carriers. This means that the wave-function of the electrons in the energy transition QD0 do not overlap with others, or in other terms, the electrons in QD0 are trapped and cannot move vertically through the dots. On the other hand, QD1→QD3 transitions have a value of m≈2.5 what implies the formation of energy bands instead of discrete levels for the QD-IB material, something which was expected theoretically in the IB model [10] and it is proven here for the first time. The formation of bands instead discrete levels could helps the performance of the QD-IBSCs allowing the movement of the carriers to empty dots which otherwise cannot pump electrons form their energy states to the CB.

By using eq. (1), fig. 5 shows the fitting over PR data for the transitions relating the WLs and the barrier material-substrate. The transitions denoted WL1 and WL2 are related to the splitting of heavy-hole and light-hole levels respectively. This splitting is caused by the extremely thin width of the QWs supporting the QDs [11]. The larger broadening of these two features, see Table I, when compared to samples with only one layer of QDs [12] could indicate that both signals are contributed by different WLs thicknesses coming from the ten layer stack. This evolution of WLs thicknesses have to be related with the different strain pattern which governs the QDs growth for different deposited layers. Because there exits mass transfer between the wetting layer and the dots during the growth process [13], the fluctuation in thicknesses for the WLs could alter the size of the QDs in the stack [14]. In this respect the TEM image, fig. 1, shows apparently bigger dots in the upper layers of the stack, and hence we expect to have thinner WLs supporting them.

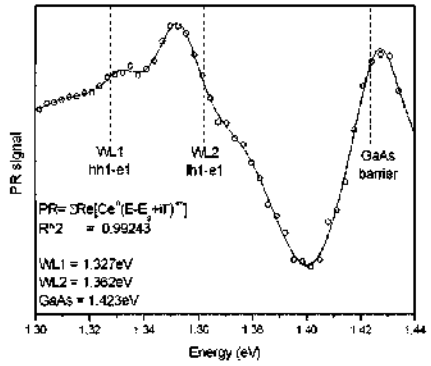

Figure 5: PR fitting procedure for WLs-barrier related signals in a QD-IBSC

The unavoidable presence of WLs during the growth of the dots in the Stranski-Krastanov growth mode degrades the performance of QD-IBSCs by adding an extra band (m_{WL}≈2.5 in Table I) offset between the IB and the CB. To overcome this problem other approaches for growing the dots can be considered (i.e. the Volmer-Webber method).

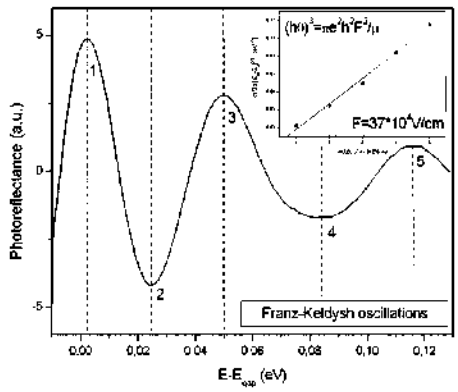

Figure 6:.FKOs fitting procedure for determining the field in the SCR for a QD-IBSC.

Another interesting feature presented in the PR spectrum of fig. 2, is the presence of FKOs [15] beyond the GaAs VB→CB transition. Under the application of a modulated electric field, the dielectric function of a semiconductor presents oscillations around the fundamental bandgap transition which can be directly monitored by PR. The period of the FKOs can be used to estimate the static electric fields presented in the sample interfaces such as the field in the space charge region (SCR) between p and n emitters. Figure 6 shows the FKOs for a QD-IBSC. By representing, see the inset Fig.

6, and fitting the energy $E-E_{gap}$ versus the index of each oscillation extrema we can extract the static electric field in the SCR. Proceeding in that way, we have obtained a figure of $37 \cdot 10^4$V/cm for the static electric field. The QDs and hence the IB material sandwiched by the p and n GaAs emitters is biased permanently. The voltage drop across the dots implies that the fermi level associated with them is not whitin the IB, in this way, the half-filling of the IB is not garanteed. In order to overcome this problem, we have proposed the use of field damping layers and/or increase the number of QDs layers in the stacks.

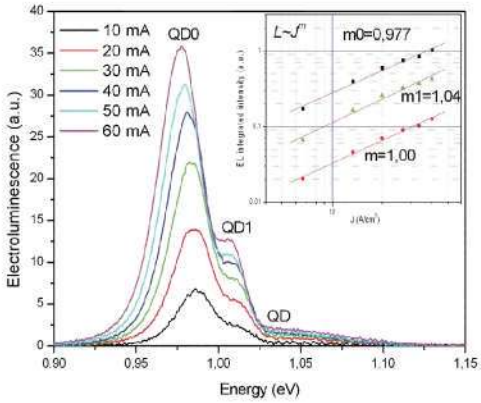

Figure 7: Characteristic EL and PR spectra for a QD-IBSC.

Another theoretical aspect covered by the ideal IBSC model is related to the radiative nature of the IB. The presence of impurity levels within the VB→CB is a well known phenomenon. In the early 60s, Wolf proposed to use these transitions for improving the photocurrent of the SCs and hence its efficiency [16]. Unfortunately these transitions have usually a non-raditive nature which implies that the levels work as traps for the carriers To overcome the trapping effect of these localized impurity levels, we have proposed to increase the concentration of impurities in order to form a band instead of discrete levels [17].

Figure 7 shows an analysis of the radiative nature of the QD-IB material for the QD0, QD1 and QD (seed layer) transitions. Studying the evolution of the integrated EL intensity as a function of the device current density we can estimate the dominating recombination nature of the transitions [18]. The dependence is characterized by $L \sim J^m$, where L is the integrated EL intensity and J is the current density. The exponent m indicates the emission mechanism of the QD-IBSC. At room temperature and current injection between 7 and 45 A/cm^2, the $L - J$ dependence, see the inset in fig. 7, displays a linear dependence ($m \approx 1$) for all the transitions under analysis, indicating that most of the injected carriers are recombining radiatively (if it is assumed that recombination takes place in the space charge region) or that recombination has shifted to the neutral regions.

The optical analysis realized over QD-IBSCs samples have shown some aspects which fit and deviate from the ideal operation of these devices. Supporting the IB model we have proved the formation of IBs and the radiative nature of them. Against the operation performance of the IBSCs, we have observed the presence of more than one IB within the bandgap of the host material; the existence of a band offset due to the WLs; and the bias of the QD-IB material immersed in the SCR between p and n emitters.

4 CONCLUSSIONS

In this paper we have characterized the optical transitions for InAs/GaAs QD-IBSCs by fitting procedures over EL and PR spectra. Good sample structural quality has been observed by TEM. By fitting PR data, we have indentified the coexistence of intermediate bands and discrete energy levels coming from the QD-IB material. The PR data evidenced also a strong electric field over the dots due to the SCR created between the p-n emitters sandwiching the IB material. Also we demonstrated the radiative nature of the IB material related energy transitions.

ADKNOWLEDGEMENTS

This work has been supported by the European Commission, the Spanish National Programme, and the Comunidad de Madrid under the contracts IBPOWER (211640), GENESIS FV (CSD2006-00004), and NUMANCIA (S-0505/ENE000310), respectively. DFM acknowledges financial support from the Spanish Ministry of Science and Innovation within the program Ramón y Cajal.

REFERENCES

[1] A. Luque, A. Martí, Phys. Rev. Lett. 78 (1997) 5014.
[2] A. Martí et al., Thin Solid Films 516 (2008) 6716.
[3] D. Bimberg, M. Grundmann and N.N. Ledentsov in *"Quantum Dot Heterostructures"*, John Wiley & Sons, UK (1998).
[4] J. Misiewicz et al., Materials Science 21 (2003) 263.
[5] S. Fafard et al., Appl. Phys. Lett. 65 (1994) 1388.
[6] S. Raymond et al., Phys. Rev. B 54 (1996) 11548.
[7] Q. Xie et al., Phys. Rev. Lett. 75(13) (1995) 2542.
[8] D. E. Aspnes, Surface Science 37, (1973) 418.
[9] H. Shen et al., Phys. Rev. B 37, (1988) 10919.
[10] A. Martí and A. Luque in *"Next generation photovoltaics, hihg efficiency trough full spectrum utilization"*, Series in Optics and Optoelectronics, Institute of Physics Publishing, Bristol (2003).
[11] S. H. Pan et al., Phys. Rev. B 38(5) (1988) 3375.
[12] G. Sek et al., J. Appl. Phys. 100 (2006) 103529.
[13] T. R. Ramachandran et al.,, Appl. Phys. Lett. 70 (1997) 640.
[14]O. G. Schmidt et al., Appl. Phys. Lett. 74, (1999) 1272.
[15] H. Shen and M. Dutta, J. Appl. Phys. 78(4) (1995) 2151.
[16] M. Wolf, Proc. IRE 48, (1960) 1246.
[17] A. Luque et al., Physica B 382 (2006) 320.
[18] W.H. Chang et al., Appl. Phys. Lett. 84(14) (2003) 2958.